2011-1

Novel Tissue Mimicking Materials for High Frequency Breast Ultrasound Phantoms

L. Cannon
Dublin Institute of Technology

Andrew Fagan
Centre for Advanced Medical Imaging, St. James's Hospital / Trinity College Dublin

Jacinta Browne
Dublin Institute of Technology, jacinta.browne@dit.ie

Recommended Citation

Browne, J. E. (2011) Novel Tissue Mimicking Materials for High Frequency Breast Ultrasound Phantoms. *Ultrasound in Med. & Biol.* Jan. vol.37, no.1, pp. 122-35. doi:10.1016/j.ultrasmedbio.2010.10.005

Title: Novel tissue mimicking materials for high frequency breast ultrasound phantoms

Author 1: Louise M Cannon (Corresponding Author)

Institutional affiliation: Medical Ultrasound Physics and Technology group, School of Physics, Dublin Institute of Technology

Address: School of Physics, Dublin Institute of Technology, Kevin Street, Dublin 8, Ireland

Email: Louise.cannon@dit.ie

Telephone: 0863933061

Author 2: Andrew J Fagan

Institutional affiliation: Centre for Advanced Medical Imaging, St. James's Hospital, Dublin

Author 3: Jacinta E Browne

Institutional affiliation: Medical Ultrasound Physics and Technology group, School of Physics, Dublin Institute of Technology

Abstract

The development and acoustical characterisation of a range of novel agar-based tissue mimicking material (TMMs) for use in clinically relevant, quality assurance (QA) and anthropomorphic breast phantoms are presented. The novel agar-based TMMs described in this study are based on a comprehensive, systematic variation of the ingredients in the International Electrotechnical Commission (IEC) TMM. A novel, solid fat-mimicking material was also developed and acoustically characterised. Acoustical characterisation was carried out using an in-house scanning acoustic macroscope at low (7.5 MHz) and high frequencies (20 MHz), using the pulse-echo insertion technique. The speeds of sound range from 1490 to 1570 m. s^{-1}, attenuation coefficients range from 0.1 to 0.9 dB. cm^{-1}. MHz^{-1} and relative backscatter ranges from 0 to - 20 dB. It was determined that tissues can be mimicked in terms of independently controllable speeds of sound and attenuation coefficients. These properties make these novel TMMs suitable for use in clinically relevant QA and anthropomorphic phantoms, and would potentially be useful for other high frequency applications such as intra-vascular and small animal imaging.

Keywords: Breast Phantom, Tissue Mimicking Materials, Speed of Sound, Attenuation, Backscatter, High Frequency

Introduction

Advances in transducer technology and system electronics, coupled with real-time image processing techniques, have continued the rapid pace of improvement evident in diagnostic ultrasound image quality in recent years. This improvement has resulted in the increased use of ultrasound in diagnostic imaging, to the level where currently accounts for 25 % of all imaging procedures worldwide (Wells2006). One particular area where ultrasound is being used more frequently is breast imaging, where it plays many important roles in both symptomatic breast imaging and breast screening, for example distinguishing benign lesions from malignant lesions and guidance of interventional procedures. The detection and diagnosis of a lesion during a breast ultrasound examination is dependent on two factors. The first factor is the instrumentation used: breast ultrasound examinations require high quality instrumentation that consistently produces high quality images, and hence routine quality assurance (QA) is necessary to ensure that scanners used for this purpose continue to produce images of the requisite high quality. The second limiting factor is the training, experience and skills of the operator. The detection and diagnosis of a lesion in a breast ultrasound examination is determined largely subjectively by the operator, and therefore there is an increasing need for the operator to be appropriately trained and skilled. However, both of these limiting factors may be overcome with the use of clinically relevant QA phantoms and anthropomorphic training phantoms. The intention of this study was to develop and acoustically characterise agar-based tissue-mimicking materials (TMMs), with acoustic properties representing a range of tissue types found in the breast (for example, subcutaneous fat, glandular tissue and pectoral muscle), suitable for use in the construction of clinically relevant QA phantoms and anthropomorphic training phantoms.

Ideally, QA and performance testing of diagnostic ultrasound scanners should allow one: to ensure that equipment performs to an agreed standard and is fit for purpose; to assess

new imaging modalities and signal processing techniques; to inform decision making in the procurement and replacement of equipment; to assist in the design of ultrasound transducers (Pye et al.2004); to correlate the QA performance of the scanner with its perceived clinical performance (Shaw and Hekkenberg2007). However, these ideals are not satisfactorily achievable with commercially available QA phantoms, as they have a number of significant limitations, in particular the TMMs used in their production and their simplistic design (Browne et al.2004).

Commercially available phantoms are all similar in design, consisting in general of nylon filaments and tissue mimicking cylindrical objects (representing anechoic and contrast structures) embedded in a homogeneous tissue mimicking background material. Previous studies have used such commercial phantoms to determine if clinically reported improvements in image quality, with new imaging technologies, could be demonstrated (Browne et al.2004;Browne et al.2005). One objective study comparing tissue harmonic imaging (THI) with conventional B-mode imaging found that some of the clinically reported improvements in image quality were not observed experimentally using these commercial phantoms (Browne et al.2004). The authors postulated that this may have been due to the simplistic homogeneous phantom design and absence of complex structures such as skin and fat layers. Another study comparing THI to conventional B-mode imaging investigated the use of a subcutaneous pig fat layer with a commercial phantom to introduce the phase aberrations and beam distortions, which would be found clinically (Browne et al.2005). Improvements with THI compared to B-mode imaging in some image parameter tests, such as anechoic target detectability, were found and these findings correlated to those reported clinically. However, this was not the case for all image parameters, in particular there was no improvement in contrast resolution, which the authors attributed to the insufficiently challenging nature of the contrast targets embedded in the phantom. Nevertheless, this study

showed that the introduction of clinically relevant materials, to represent complex tissue structures, can enable one to correlate image quality to the perceived clinical performance.

Ultrasound scanners are based on a number of assumptions, when these assumptions are not met artifacts are likely to be produced in the image, for example, reverberation, partial volume and refraction artifacts. Some of the most deteriorating artifacts in ultrasound images are due to differences in the speed of sound of the propagating medium, as ultrasound images are formed assuming a constant speed of sound (1540 m. s^{-1}). In reality, there is a significant variation in the speed of sound *in-vivo*; for example, the speed of sound varies from 1470 m. s^{-1} in fatty tissues to over 1600 m. s^{-1} in muscle and up to 3700 m. s^{-1} in bone. This variation in speed of sound results in phase aberrations and beam distortions (Wells1975) and effectively leads to image artifacts and mis-registration of anatomical structures. Breast ultrasound imaging is particularly susceptible to image artifacts due to the range of tissues with varying speed of sounds present in the breast.

The most common TMMs used in commercial phantoms are gelatine, evaporated milk, agar, urethane rubber and Zerdine™, the manufacturers of these materials quote speeds of sound of approximately 1540 m. s^{-1} (with the exception of urethane-rubber which has a speed of sound of 1460 m. s^{-1}) and attenuation coefficients of either 0.5 or 0.7 dB. cm^{-1}. MHz^{-1}. An independent study assessing the acoustic properties of these TMMs characterised their speed of sound, attenuation coefficient and relative backscatter properties with increasing frequency (2 to 15 MHz) and increasing temperature (10 to 35 ºC) (Browne et al.2003). The measured speeds of sound for all TMMs were found to be frequency independent while the attenuation coefficient of all the TMM increased with increasing frequency. With the exception of the agar-based material, all of the TMMs exhibited a non-linear response of attenuation with frequency, in particular, urethane rubber TMMs exhibited a highly non-linear response across this frequency range. This property would lead to

deterioration in penetration depth performance and axial resolution at frequencies higher than 7 MHz (Chen and Zagzebski2004;Goldstein2000), rendering it unsuitable for use in high frequency applications. The agar-based TMM was the only material to exhibit a linear response of attenuation with frequency (approximately $f^{1.01}$). The acoustic properties of all TMMs varied with temperature, with the minimum variation observed in the agar-based TMM. To date the agar-based material is the only TMM which has been acoustically characterised at high frequencies (17 to 23 MHz). At these high frequencies its speed of sound was found to be independent of frequency and the attenuation coefficient was found to have a linear response to frequency (Brewin et al.2008). Another study on this agar-based TMM showed that a limited variation of the scattering ingredients during the manufacturing process resulted in TMMs with varying attenuation and backscattering properties (Inglis et al.2006). This study showed that the acoustic properties of this TMM can be adjusted, an important feature which highlights the potential for varying the acoustic properties of this material by adjusting its ingredients. However, a limitation of the study was that all ingredients were varied simultaneously, and hence the effect of individual ingredients on the resulting acoustic properties remains unknown.

Unlike other imaging modalities, an ultrasound scanner should not be evaluated solely by its ability to resolve closely spaced point targets namely, spatial resolution. Rather, it is more important to be able to detect small, negative contrast, anechoic regions surrounded by speckle, this feature is particularly important in breast imaging as it determines the system's ability to detect low contrast cysts and lesions. As previously stated, performance assessment should ideally allow one to correlate QA performance with its perceived clinical performance. At present, commercially available phantoms are not fit for this purpose due to the acoustic properties of the TMMs used in their production. The TMMs are homogeneous and have a uniform speed of sound of 1540 m. s^{-1}, hence, the artifacts introduced in a clinical

situation would not be present and tests performed could not be realistically compared to clinically reported findings. Therefore, whilst commercial phantoms may be useful for undertaking consistency checks such as axial and lateral resolutions, their acoustic properties and simplistic design do not allow us to correlate QA with perceived clinical performance. For clinical performance *in-vitro* testing of an ultrasound scanners performance the QA phantom TMMs must have the same range of speeds of sound, attenuation coefficients and backscatter, as the organ they aim to mimic, only then can the true clinical situation be simulated and the scanners performance in the presence of clinical artifacts be evaluated.

Furthermore, it is essential that these acoustic properties remain consistent for the range of frequencies used diagnostically. Unlike applications such as abdominal or foetal imaging, which are low frequency applications (typically < 5 MHz); breast imaging is a high frequency application. Low frequencies are utilised in order to seek a compromise between resolution and penetration depth, however, no such compromise is required for breast ultrasound. When the breast is imaged in the supine position, the mammary zone typically lies at a depth of 1 to 4 cm from the face of the transducer. Most pathology arises in the mammary zone of the breast, so high resolution is imperative in this region, therefore, high frequency transducers are utilised. In recent years, with improvements in transducer technology, the frequency of transducers employed in breast imaging has seen an increase, for example, the Philips iU22 L17-5 (Philips Healthcare, Andover, MA, USA) linear array, which has a frequency bandwidth of 5 to 17 MHz, and the Siemens Acuson S2000™ 18L6 HD (Siemens Healthcare, Erlangen, Germany) transducer, which has a frequency bandwidth of 5.5 to 18 MHz.

This study describes the production and characterisation of a number of TMMs, which are based on a systematic variation of the ingredients in the agar-based IEC TMM in order to determine in detail their effects on the overall acoustic properties of the TMMs.

Furthermore, the manufacturing process for novel oil-in-agar based TMMs for mimicking subcutaneous fat is also described. Finally, in this study an approach to predicting the optimum ingredients and their relative proportions to produce long-term stable TMMs, suitable for use in high frequency breast ultrasound phantoms, is suggested.

Materials and Methods

Tissue Mimicking Materials

The components of the IEC TMM and their percentages by weight are given in Table 1 (IEC1996;Teirlinck et al.1998). To produce the TMM, the liquid components (water, glycerol and benzalkonium chloride) were mixed together in a stainless steel container. The dry components (agar, SiC (17 μm), Al_2O_3 (3.0 μm) and Al_2O_3 (0.3 μm)) were then added to the liquid mixture. A commercial hand blender (HR1363, Philips, Amsterdam, Netherlands) was then used to thoroughly mix the ingredients and ensure even particle dispersion. The stainless steel container was then place in a heated water bath at 96 ºC and an electronic stirrer was inserted in the mixture to maintain even particle dispersion. A Fluke multimeter with an integrated temperature probe (Fluke 16, Eindhoven, Netherlands) was used to monitor the temperature of the mixture, and when the temperature exceeded 90 ºC the time was recorded and the TMM mixture remained in the water bath for exactly 1 hour thereafter. The mixture was then removed from the water bath and allowed to cool at room temperature, while being stirred at 75 rpm. When the temperature of the TMM had cooled to 46 ºC it was injected into a pre-cut cylindrical perspex mould (Fig. 1). The side of the mould was sealed with a layer of saran wrap® attached using araldite adhesive (Araldite® 2012, Huntsman Advanced Materials, Switzerland). Each mould had two ports, a TMM injection port and an air exhaust port to allow air to escape when injecting the TMM. The use of the saran wrap layer prevented diffusion of glycerol during acoustical testing of the TMMs, and also

prevented the TMMs from desiccating when they were left to stand at room temperature during acoustic testing. However, for long-term storage, the TMMs were kept in an air tight container with a mixture of water (87.67 %)/glycerol (11.84 %)/benzalkonium chloride (0.48 %) at room temperature. This mixture restores the concentration of glycerol component to the TMM, keeps the TMM samples hydrated and prevents bacterial invasion (Brewin et al.2008).

Table 1. Weight composition of the TMM (by %)

Component	Weight composition (%)
Distilled, degassed, deionised water	82.97
Glycerol	11.21
Benzalkonium chloride	0.46
Agar	3.00
Silicon carbide (17 μm)	0.53
Aluminium oxide (3.0 μm)	0.95
Aluminium oxide (0.3 μm)	0.88

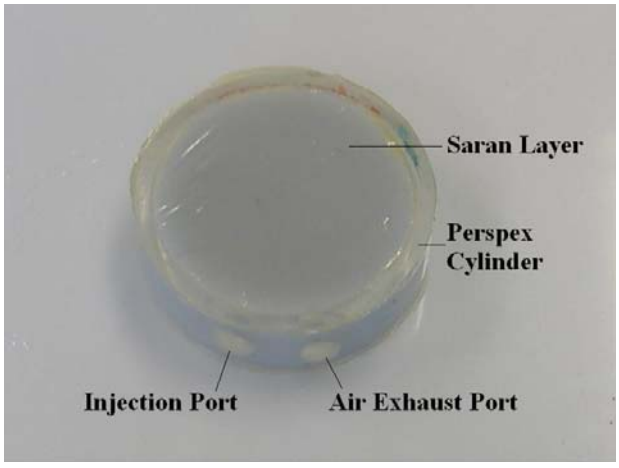

Fig. 1. Cylindrical mould for TMMs

An empirical study was carried out to quantify the change in acoustic properties with glycerol, Al_2O_3, and SiC as well as determining their respective interrelationships. Four of

the TMMs' key ingredients were investigated separately, namely: "series 1" - glycerol; "series 2" SiC (17 μm), Al_2O_3 (0.3 μm) and Al_2O_3 (3 μm); "series 3" Al_2O_3 (0.3 μm) and Al_2O_3 (3 μm); and "series 4" SiC (17 μm). Furthermore, a solid fat mimicking material was developed and acoustically characterised ("series 5"). The component(s) varied and their percentage concentration in each series are summarised in Table 2. In series 1 different percentage concentration of glycerol were used to adjust the speed of sound (from no glycerol, 0 %, to the concentration of glycerol in the original TMM, 100 %, to 50 % more glycerol than that in the original TMM, 150 %). In series 2, the percentage concentration of the TMM particles, SiC, Al_2O_3 (0.3 μm) and Al_2O_3 (3 μm), were varied to adjust the attenuation coefficient and relative backscatter. In series 3, the percentage concentration of Al_2O_3 (0.3 μm) and Al_2O_3 (3 μm) were varied to adjust the attenuation. In series 4, the percentage concentration of SiC was varied to adjust the backscatter. In series 5, an olive oil and surfactant mixture was added to the original TMM to produce a solid fat-mimicking TMM. The fat-mimicking TMM was produced as follows. Olive oil (90 %) and surfactant (10 %) were thoroughly mixed together using the hand blender. The surfactant used was Synphronic N (Conservation Resources, Oxford, UK) which was diluted to 10 % in degassed, distilled, deionised water. The olive oil/surfactant mixture was heated to 96 ºC and added to molten TMM (that is, IEC TMM which had been boiled at 96 ºC for 30 minutes). The entire mixture remained in the heated water bath for a further 30 minutes. It was necessary to heat the olive oil/surfactant mixture to 96 ºC as this prevented the molten agar from congealing following their addition to the mix.

Table 2. Variation of the IEC ingredient concentrations used in this study

	Component (s) varied	Concentrations (%)
Series 1	Glycerol	0 and 50 – 150 in steps of 10
Series 2	SiC, Al_2O_3 (0.3 μm) and Al_2O_3 (3 μm)	0 – 20 in steps of 5, 30 – 60 in steps of 10, 75 and 100 – 200 in steps of 20
Series 3	Al_2O_3 (0.3 μm) and Al_2O_3 (3 μm)	100 – 200 in steps of 10 and 250
Series 4	SiC (17 μm)	50 -100 in steps of 10
Series 5	Olive Oil and Surfactant	0 – 30 in steps of 5

Acoustic Characterisation

Scanning Acoustic Macroscope

All acoustic tests were carried out using a Scanning Acoustic Macroscope (SAMa) system developed in-house (Fig. 2). This was developed using a pulser receiver (Model 5052PR, Panametrics, USA), a linear actuator, a data acquisition card (PCI – 5144, National Instruments, USA) and the programming environment LabView (National Instruments, USA). Two broadband immersion transducers were available for use with this system. These broadband transducers had frequencies centered at 7.5 MHz (Panametrics V320-SU, Olympus NDT Inc, Waltham, MA, USA) and 20.0 MHz (Panametrics V317-SU, Olympus NDT Inc, Waltham, MA, USA). The properties of these transducers are given in Table 3.

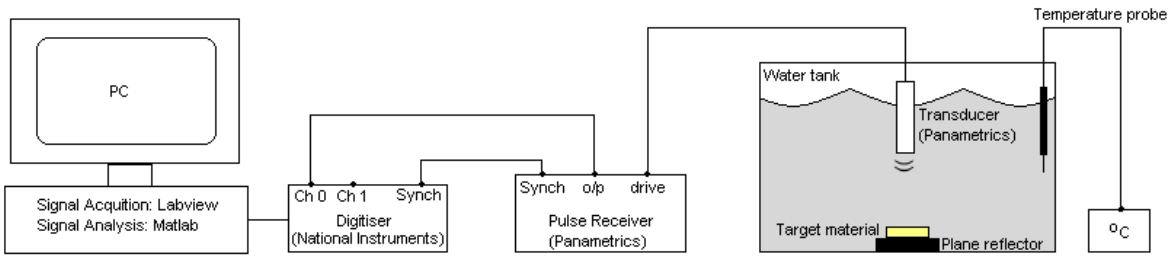

Figure 2 *Scanning acoustic macroscope configuration*

Table 3. Properties of the transducers used in this study

Transducer (MHz)	Frequency Range (MHz)	Focal Point (cm)	Crystal Diameter (mm)
7.5	5.15 – 9.44	9.54	12.7
20	14.84 – 24.50	6.55	6.35

The SAMa was operated in pulse-echo configuration for the acoustic testing. In this configuration a single transducer acted as both a transmitter and a receiver. This transducer was positioned in a tank of degassed water, with the focus on the surface of the bottom of the tank, where the glass bottom acted as a plane reflector. The movement of the transducer was controlled by a linear actuator, programmed to advance the transducer laterally over a 1 cm area on the reflector. At each 1 mm advance the transducer was pulsed, and the resulting pulse was transmitted through the degassed water and reflected from the glass plate. The reflected pulse was subsequently detected by the transducer, digitised and stored as part of a data set for off-line analysis using custom software (MATLAB 2007b, The MathWorks Inc., USA). For each acoustic measurement two data sets were required, a reference data set and a sample data set. The reference data set was acquired from a scan of the plane reflector. The sample data set was acquired from a scan of the reflector with the TMM sample positioned in the space between the transducer and the reflector. All acoustic measurements were performed in degassed water at 20 ± 0.5 ºC.

Speed of Sound

To measure the speed of sound of the TMMs the custom software calculated the time difference of the peaks (the time shift, Δt) of the RF pulses from the reflector with and without the sample in place. When the sample was not in place a perspex mould filled with degassed water was placed between the transducer and the reflector. The perspex mould contained 2 saran wrap® layers, thereby ensuring that their effect on the acoustic

measurement of the TMM sample was accounted for in the measurement. The speed of sound of the sample, c_s, was then calculated using Equation 1 (AIUM1995):

$$c_s = \frac{c_w}{1 + \Delta t \frac{c_w}{2d}} \qquad \text{Equation 1}$$

where d is the thickness of the sample, c_w is the speed of sound in water and Δt is the measured time shift. Two samples of each TMM were produced for acoustic testing. Three data sets from each of the samples were acquired, from each data set 10 measurements of speed of sound were computed.

Attenuation Coefficient

The attenuation coefficient was calculated by performing a fast Fourier transform (FFT) on the RF signals from the plane reflector with and without the sample in the path. The attenuation coefficient, α, in dB. cm^{-1} was calculated from the log difference between the spectra, using Equation 2 (AIUM1995):

$$\alpha(f) = -\frac{20}{2d} \log_{10} \frac{A(f)}{A_0(f)} \qquad \text{Equation 2}$$

where d is the sample thickness, $A(f)$ is the sample magnitude spectrum at frequency f and $A_0(f)$ is the reference magnitude spectrum at frequency f. The effect of the saran wrap was accounted for by acquiring the reference signal with a cell containing degassed water bound by saran wrap® in the path.

Relative Backscatter Power

For the relative backscatter power measurement the acquisition of the sample RF signal required a different set-up to that used for speed of sound and attenuation coefficient measurements. In this case, the signal of interest was the backscattered RF signal, captured between the front face of the sample and the plane reflector. Therefore, the transducer was adjusted to position the focus of the ultrasound beam 1 mm below the surface of the sample

and the drive voltage of the transducer was increased to 240 V. These adjustments minimised interference caused by the reflection from the front face of the sample and improved the signal to noise ratio of the backscattered RF signal.

The backscattered RF sample signal was saved for offline analysis using custom software as follows: the RF signal was windowed, this windowed section contained the RF signal from a section approximately 1mm below the surface of the sample. This signal was segmented into eight sections of equal length, each with 50 % overlap. Each segment was then windowed with a Hamming window that was the same length as the segment, to optimize frequency resolution, in advance of a spectral analysis of the power density using the Welch transform (Welch1967). The Welch transform derives the distribution of power per unit frequency in the backscattered RF signal, normalized to the total received power, by averaging the spectra from all segments (Brewin et al.2008). The power spectrum, I_o, of the reference RF signal was computed and the relative backscatter, μ, of the sample was then computed using Equation 3:

$$\mu(f) = -10\log_{10}\frac{I(f)}{I_0(f)} \qquad \text{Equation 3}$$

Validation of Acoustic Measurements

Measurements of speed of sound and attenuation coefficients were validated using a silicon oil reference cell supplied by the UK National Physical Laboratory (NPL, Teddington, UK). The test cell was 1cm thick and had a known attenuation coefficient between 1 to 10 MHz at a temperature of 21.5 ºC. Results of attenuation as a function of frequency for the NPL test cell are shown in Fig. 3. Measured values for attenuation were found to match those reported by the NPL. The NPL stated the speed of sound for reference cell at 7 MHz was 1382 ± 14 m. s^{-1}. The SAMa system measured a speed of sound of 1385 m. s^{-1}, at 21.5 ºC, this was within 0.2 % of the NPL measurement.

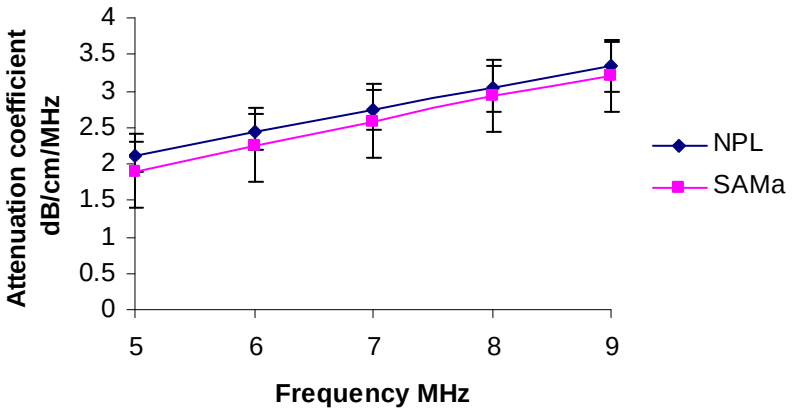

Fig. 3. Attenuation coefficient of the NPL reference cell as a function of frequency

Density and Impedance Measurements

For determination of the IEC, series 1 and series 5 TMM densities, the mass of each TMM with a defined volume was measured. Knowing the densities and acoustic velocities, acoustic impedances, z, were calculated according to:

$$z = \rho_0 c_s \qquad \text{Equation 4}$$

where ρ_0 is the density of the TMM sample and c_s is the speed of sound of the TMM sample.

Results

Five series of TMMs were developed and the acoustical properties were measured. The speeds of sound and attenuation coefficients of each of the samples were measured with frequencies of 7.5 and 20 MHz at 20 ºC. No particle sedimentation was evident in any of the TMMs produced and to date, the preservation measures used for the TMMs (that is, immersed in a mixture of glycerol, water and Rodalon™ in a high density polyethylene container with an airtight lid) have been found to be successful with the sample being preserved for over 6 months.

In series 1, samples with different glycerol concentrations were produced to determine the effect of glycerol on the speed of sound of the TMM. The variation of the speed of sound as a function of increasing glycerol concentration (at frequencies of 7.5 MHz and 20 MHz) is shown in Fig. 4, where it can be seen that the speed of sound increased across the range 1490 to 1568 m. s^{-1} with increasing concentration of glycerol. The attenuation coefficient remained constant with increasing glycerol concentration. It was also found that the effect of transmit frequency on the speed of sound and attenuation coefficient was negligible. The effect of the glycerol concentration on the density and impedance properties of these TMMs was also investigated, these results can be viewed in Fig. 5. The results show that the concentration of glycerol had no significant effect on either property, as all data points were within experimental variation.

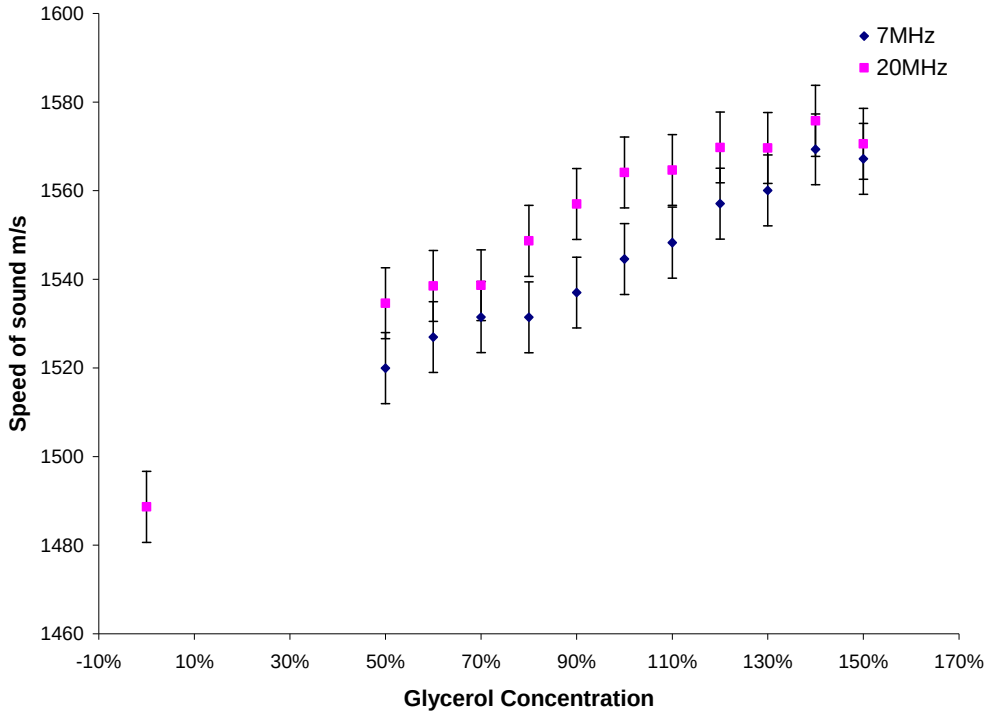

Fig. 4. Effect of glycerol concentration on the speed of sound (± 10 m. s^{-1}) of the TMMs

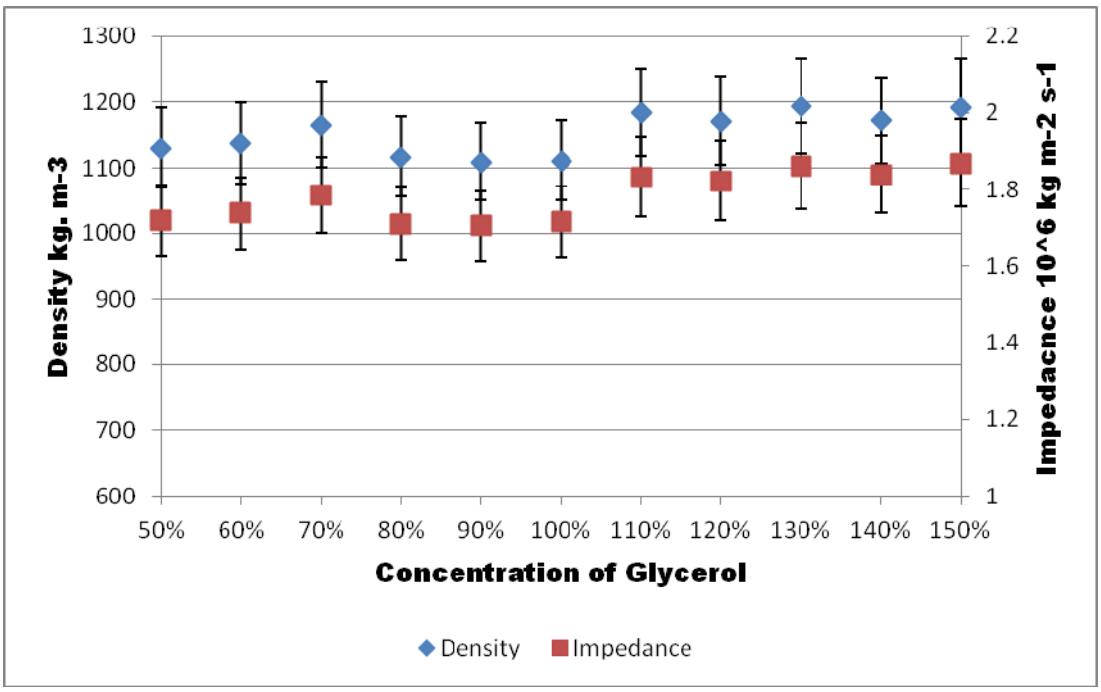

Fig. 5. Effect of glycerol concentration on the density and impedance of the TMMs

In series 2, the effect of varying the concentration of the TMM particles SiC, Al_2O_3 (0.3 µm) and Al_2O_3 (3 µm) on the attenuation coefficient and the relative backscatter are

presented in Fig. 6 and 7 respectively. The attenuation coefficient was found to increase from 0.1 to 0.8 dB. cm^{-1}. MHz^{-1} with increasing particulate concentration, with no appreciable difference measured for both frequencies tested, which indicates a linear dependence of attenuation coefficient with frequency. The backscatter of the TMMs ranged from 0 to - 20 dB relative to the original TMM (that is, 100 % particulate concentration). The particulate concentration of the TMMs exhibited no effect on their resulting speed of sound, the average speed of sound was 1551 ± 10 m. s^{-1}.

Fig. 6. Effect of SiC, Al_2O_3 (0.3 μm) and Al_2O_3 (3 μm) concentration on the attenuation coefficient (± 0.03 dB. cm^{-1}. MHz^{-1}) of the TMMs at 20 ºC

Fig. 7. Effect of SiC, Al_2O_3 (0.3 μm) and Al_2O_3 (3 μm) concentrations on relative backscatter (± 3 dB) of the TMMs at 20 ºC

In series 3, the Al_2O_3 (0.3 μm and 3 μm) particulate concentration was varied to determine its individual effect on the resulting attenuation coefficient and speed of sound of the material. The attenuation coefficient is plotted as a function of increasing Al_2O_3 concentration for both 7.5 and 20 MHz frequencies in Fig. 8. The attenuation coefficient was found to increase from 0.5 to 0.9 dB. cm^{-1}. MHz^{-1} with increasing particulate concentration, with no appreciable difference measured for both frequencies tested, which indicates a linear dependence of the attenuation coefficient with frequency. The Al_2O_3 particulate concentration did not alter the speed of sound of the TMMs: the average speed of sound of the TMMs was 1548 ± 10 m. s^{-1}.

In series 4, samples with varying SiC concentrations were produced to determine the effect of SiC on the attenuation coefficient, relative backscatter and speed of sound of the TMMs. A graph of attenuation coefficient as a function of SiC concentration is presented in

Fig. 9 for 7.5 and 20 MHz frequencies, where it is evident that this variation of SiC concentration has no effect on the measured attenuation coefficient at either frequency. The average attenuation coefficient measured with a frequency of 7.5 MHz was 0.44 dB. cm^{-1}. MHz^{-1} and with 20 MHz was 0.55 dB. cm^{-1}. MHz^{-1}. Therefore, an attenuation coefficient with non-linear frequency dependence is apparent for these TMMs. The speed of sound and relative backscatter values remained the same for each concentration of SiC.

In series 5, varying concentrations of an oil surfactant mixture were added to the original TMM mixture in order to investigate its potential as a fat TMM. The measured speeds of sound of the TMMs as a function of oil surfactant concentration are presented in Fig. 10, where it is evident that increasing oil concentration reduces the speed of sound of the TMM. The measurements of speed of sound range from 1482 to 1543 m. s^{-1}, with a standard deviation of ± 10 m. s^{-1}. The attenuation coefficient of each sample was measured and plotted as a function of oil surfactant concentration in Fig. 11. The oil concentration does not appear to directly affect the attenuation coefficient which was centered around 0.5 dB. cm^{-1}. MHz^{-1}, with the exception of the TMM with 40 % oil concentration, which exhibited an attenuation coefficient of 0.6 dB. cm^{-1}. MHz^{-1}. The density and impedance properties of this potential fat TMM were also investigated, each of these properties are plotted as a function of oil concentration in Fig. 12. These results demonstrate that the concentration of oil in the samples no significant effect on either density or impedance of the resulting TMMs.

Discussion

Specific clinical performance testing of diagnostic medical ultrasound scanners requires complex QA phantoms. At present, commercially available phantoms are not fit for this purpose due to their simplistic design and the properties of the TMMs used in their

production, although manufacturers, such as CIRS Inc. have been known to produce custom designs. However, the specific design criteria and results pertaining from these custom built phantoms are not widely known nor have they been reported in the scientific literature. The TMMs (background and targets) used in currently available commercial phantoms are homogeneous in terms of speed of sound and attenuation. Their embedded targets differ from the surrounding background tissue in terms of backscatter; however, the level of difference in backscatter is insufficiently challenging to the scanner, with targets typically exhibiting backscattering ranging from - 12 dB to + 12 dB in, at best, 3 dB steps. Therefore, whilst these phantoms may be useful for consistency checks such as spatial resolutions, more complex QA phantoms are required for testing the clinical performance of the scanner. These more complex phantoms must contain tissue mimicking materials which represent the range of speeds of sound, attenuation coefficients and relative backscatter values typically found in the clinical situation. Suitable TMMs would be required to simulate anatomical structures and embedded targets, and also allow for the introduction of artifacts which are inherent in medical ultrasound, for example, artifacts related to refraction and reflection at fat to non-fat interfaces.

In this study, a range of agar-based TMMs were developed and acoustically characterised to determine if they would be suitable for use in high frequency breast ultrasound phantoms. The range of acoustic properties found in some of the tissues of the breast can be viewed in Table 4. These novel TMMs are based on a systematic variation of the ingredients of the IEC TMM (IEC1996;Teirlinck et al.1998). By performing this systematic variation of the ingredients, a wide range of materials with different attenuation coefficients, speeds of sound and relative backscatter values were manufactured. The pure IEC agar-based TMM was selected for use in this study as it has been reported to maintain its acoustic properties over a two-year period, also its acoustic properties have been

characterised at high frequencies centered around 20 MHz (Brewin et al.2008). Furthermore, a previous study showed that a limited variation in the particulate ingredients of this material produced materials with different attenuation coefficients and relative backscatter values (Inglis et al.2006).

The transducers used in this study had central frequencies of 7.5 and 20 MHz and frequency bandwidths of 5.15 to 9.44 MHz and 14.84 to 24.50 MHz respectively. These frequencies were chosen as they correspond to a range of implemented frequencies used in state-of-the-art breast ultrasound systems. The inclusion of two further transducers with central frequencies of 10 MHz and 15 MHz would have been optimal as this would encompass the entire range of frequencies utilised in breast imaging. Nevertheless, the transducers utilised were able to demonstrate the effect of low and high frequencies on the attenuation coefficients and the speed of sounds of the newly developed TMMs. Thus, these results are not only relevant for breast ultrasound applications but also in other high frequency applications such as intra-vascular studies and the new field of high frequency small animal imaging. In addition, the use of these transducers allowed an intra-laboratory cross-check with the results for the standard IEC TMM published by (Browne et al.2003, Inglis et al.2006 and Brewin et al.2008).

In this study, it was found that by altering the glycerol component of the TMM, the speed of sound could be altered independently of attenuation coefficient. This result was expected as the speed of sound of pure glycerol is 1923 m. s^{-1} (Dymling et al.1991) and the speed of sound of pure water-based agar is 1482 m. s^{-1} (Del Grosso and Mader1972), therefore the increase in the concentration of glycerol would serve to increase the overall speed of sound of the TMM. Nevertheless, these data are significant as they can act as a reference for selecting a preferred speed of sound. The range of speeds of sounds measured was 1490 to 1567 m. s^{-1}. Materials in this range have the potential to mimic a number of

tissues within the breast in terms of speed of sound, namely glandular tissue, pectoral muscle and malignancies. Furthermore, the addition of increasing concentration of glycerol may further increase the speed of sound to higher values necessary to mimic that of a fibroadenoma within the breast. The concentration of glycerol exhibited no significant effect on the density and impedance of the TMMs. The density and impedance values for IEC TMM (100 % glycerol concentration) demonstrated good interlaboratory agreement with those reported in previous studies (Brewin et al.2008;Zell et al.2007). With the significant increase in speed of sound, c_s, it was expected that there would be a corresponding increase in impedance, z, for the TMMs as $z = \rho_s c_s$. This expectation was proved incorrect as the concentration of glycerol exhibited no significant effect on either the impedance or the density, ρ_s, of the TMMs. Therefore, it is assumed that increasing the glycerol must effect the adiabatic bulk compressibility, κ, of the resulting TMM as a significant change in speed of sound was demonstrated and $c_s = \frac{\sqrt{1}}{\rho_0 \kappa}$. The preferred method for measuring density is Archimedes principle (buoyancy method) (Rosin et al.2002). Our method for measuring density was that reported by (Zell et al.2007) and our results are comparable. Furthermore, our results for the IEC TMM compare favorably with those reported by (Brewin et al.2008), who utilised Archimedes principle.

A range of TMMs with varying attenuation coefficients and relative backscattering were produced using a systematic variation of the SiC, Al_2O_3 (0.3 µm) and Al_2O_3 (3 µm) particulates. The minimum attenuation coefficient that can be achieved with no particles in the TMM is 0.1 dB. cm^{-1}. MHz^{-1}. A systematic increase of the particulate concentration was found to result in a corresponding increase in attenuation coefficient. An increase in attenuation coefficient was expected as Al_2O_3 has been reported to predominantly contribute to the value of attenuation coefficient (Inglis et al.2006). Measured data in the 0 to 100 % particulate concentration compare favourably to those measure in a previous study by Inglis

et al. (2006). These data are significant as they shows that any value of attenuation coefficient within the range in soft body tissues can be obtained by choosing the appropriate scatterer concentrations. Another significant observation is that any value of attenuation coefficient within this range can be obtained without altering the speed of sound of the material, which was shown to be independent of scatterer concentration. The range of attenuation coefficients measured in these materials has the potential to mimic glandular, fat, areola and malignant tissues in the breast. Measurements of relative backscatter show that reducing the concentration SiC, Al_2O_3 (0.3 μm) and Al_2O_3 (3 μm) in the pure IEC TMM reduces the backscatter of the material from 0 dB to - 20 dB. This was expected as SiC has been reported to contribute to the backscatter power. The TMM with 0 % scatterers had a backscattered power that differed from the IEC TMM by 20 dB such a material has potential as a mimic for anechoic structures such as a simple cyst. Apart from two particulate concentrations (0 % and 75 %), these data are consistent to those found in the study by Inglis et al. (2006). The discrepancy with 0 % and 75 % measurements may be attributed to a number of factors. Firstly, in the study by Inglis et al. (2006) no measurement uncertainties were provided for the backscatter data presented. Secondly, a major difficulty in the measurement of backscatter is the range of methods that are available for its measurement; there is no standard method and little correlation between different methods. Finally, it has been reported that backscatter coefficient measurements are often underestimated and the authors postulated that the measurement of backscatter would benefit from the use of a common reference material (Wear et al.2005).

Increasing the concentration of the Al_2O_3 particles to determine their individual effect on the attenuation coefficient showed comparable results to those obtained when both the Al_2O_3 and SiC concentrations were varied. Again, these values of attenuation coefficient can be achieved without varying the speed of sound in the resulting TMM. Furthermore, the

range of attenuation coefficients measured in these materials has the potential to mimic glandular, fat, areola and malignant tissues of the breast.

The fact that varying the SiC particle concentration did not influence the speed of sound, attenuation coefficient or relative backscatter was not expected, since SiC has previously been reported to contribute significantly to the relative backscatter power, however, this lack on influence on backscatter may be attributed to the difficulties in measuring backscatter. Furthermore, only a limited variation of SiC concentration was investigated in the current study, with 5 samples with varying SiC particles produced and characterised ranging from 50 to 100 %.

In the breast there is a large speed of sound variation between the irregularly distributed fatty and glandular tissues. This variation in speed of sound results in phase aberrations and beam distortions and effectively leads to multiple image artifacts. Currently available commercial phantoms do not have materials which mimic the fat layer. Furthermore, there is no solid fat-mimicking material available for mimicking the subcutaneous fat layer. Previous studies have utilised olive oil, lard and pig fat as fat mimics, however, olive oil is not a solid and would have to be replaced each time QA tests are performed, lard does not have suitable acoustic properties, and the use of pig fat is inconvenient for routine testing.

The inclusion of the oil surfactant mix in the agar TMM reduced the speed of sound to a minimum of 1483 $m.s^{-1}$ at 40 % oil surfactant concentration. Inclusions of the oil surfactant mixture greater than 40 % prevented the molten TMM from congealing. A reduction in speed of sound with increasing oil concentration was expected as the speed of sound of olive oil is 1490 $m.s^{-1}$ (Browne et al.2005), so when the oil is mixed with the molten TMM it would reduce the overall speed of sound of the resulting TMM. Oil surfactant inclusions with concentrations of 40 % and 35 % are within the reported value for

subcutaneous fat. The concentration of oil did not appear to directly affect the attenuation coefficient of the TMMs. However, it is possible that the inclusion of a higher scatterer concentration could increase the attenuation coefficient of this material to the value range reported for subcutaneous fat. With the significant decrease in speed of sound, *c*, it was expected that there would be a corresponding decrease in impedance. Yet, this was not the case, as the inclusion of oil surfactant concentration demonstrated no significant effect on either the impedance or the density of the TMMs. Therefore, it is assumed that increasing the oil surfactant concentration must again affect the adiabatic bulk compressibility of the resulting TMM as a significant change in speed of sound was demonstrated.

Suitable TMMs for mimicking breast tissues are in suggested Table 4. Tissues can be produced to mimic the range of acoustic properties found in the breast. Presently, the artifacts due to changes in acoustic properties and tissues structures can only be observed in clinical B-mode images, however, the introduction of clinically relevant TMMs in QA phantoms will allow for experimental measurement of QA parameters such as contrast detectability and anechoic target detectability in the presence of clinically relevant artifacts. It is envisaged that ultrasound researchers will see the value of TMMs that can be produced to represent a range of tissue types. Especially in the area of complex QA phantom development for *in-vitro* assessment of ultrasound scanners, where the goal is to correlate QA performance with perceived clinical performance and establish performance guidelines.

Summary

The agar-based TMMs investigated in this study are suitable for use in the production of complex QA and anthropomorphic phantoms. Tissue types can be mimicked through independently controlled speeds of sound and attenuation coefficients by variation of the individual TMM components. The actual choice of material depends on which tissue type

within the body is to be simulated. The acoustic properties of the materials investigated in this work were independent of frequency in the wide diagnostic range investigated, demonstrating that they are suitable for use even in high frequency applications. Indeed, the motivation of this work was to simulate the properties of the tissue types in the breast, primarily glandular tissue, subcutaneous fat, pectoral muscle, areola and malignant and benign lesions. Materials for mimicking each of these tissues have been identified and are currently being used in the construction of complex QA and anthropomorphic phantoms. A major advantage of this range of materials is their relative ease of manufacture and the ease of controlling their acoustic properties. Furthermore, the material is robust and can be moulded into any form in the manufacturing phase using a suitable mould.

Acknowledgements

The authors would like to acknowledge Technological Sector Research Strand I for funding this study.

List of Tables

Table 1. Weight composition of the TMM (by %)

Component	Weight composition (%)
Distilled, degassed, deionised water	82.97
Glycerol	11.21
Benzalkonium chloride	0.46
Agar	3.00
Silicon carbide (17 μm)	0.53
Aluminium oxide (3.0 μm)	0.95
Aluminium oxide (0.3 μm)	0.88

Table 2. Variation of the IEC ingredient concentrations used in this study

	Component (s) varied	Concentrations (%)
Series 1	Glycerol	0 and 50 – 150 in steps of 10
Series 2	SiC, Al_2O_3 (0.3 μm) and Al_2O_3 (3 μm)	0 – 20 in steps of 5, 30 – 60 in steps of 10, 75 and 100 – 200 in steps of 20
Series 3	Al_2O_3 (0.3 μm) and Al_2O_3 (3 μm)	100 – 200 in steps of 10 and 250
Series 4	SiC (17 μm)	50 -100 in steps of 10
Series 5	Olive Oil and Surfactant	0 – 30 in steps of 5

Table 3. Properties of the transducers used in this study

Transducer (MHz)	Frequency Range (MHz)	Focal Point (cm)	Crystal Diameter (mm)
7.5	5.15 – 9.44	9.54	12.7
20	14.84 – 24.50	6.55	6.35

Table 4. Ultrasonic properties of the breast tissues & suggested mimicking materials

Tissue	Speed of Sound m. s^{-1}	Attenuation Coefficient dB. cm^{-1}. MHz^{-1}	Mimicking Material
Glandular tissue	1553 ± 35 *	2.0 ± 0.7 @ 7 MHz †	Series 1 (120 %) & Series 3 (260 %)
Subcutaneous fat	1479 ± 32 *	0.6 ± 0.1 @ 7 MHz †	Series 5 (35 %)
Pectoral muscle	1545 ± 5 ‡	---	Series 1 (110 %)
Areola	---	1.1 @ 5 MHz §	Series 3 (260 %)

Malignant lesions	1550 ± 35 *	1.0 ± 0.2 @ 7 MHz †	Series 1 (110 %) & Series 3 (260 %)
Fibroadenoma	1584 ± 27 *	---	Series 1 (140 %)

* = (Scherzinger et al.1988)

† = (D'Astous and Foster1986)

‡ = (Goss et al.1978)

§ = (Goss et al.1980)

REFERENCES

AIUM. Methods for specifying acoustic properties of tissue mimicking phantoms and objects, Stage I, Laurel, MD: American Institute of Ultrasound in Medicine Technical Standards Committee. 1995;

Brewin MP, Pike LC, Rowland DE, Birch MJ. The acoustic properties, centered on 20 MHz, of an IEC agar-based tissue-mimicking material and its temperature, frequency and age dependence. Ultrasound Med Biol 2008;34:1292-306.

Browne JE, Ramnarine KV, Watson AJ, Hoskins PR. Assessment of the acoustic properties of common tissue-mimicking test phantoms. Ultrasound Med Biol 2003;29:1053-60.

Browne JE, Watson AJ, Gibson NM, Dudley NJ, Elliott AT. Objective measurements of image quality. Ultrasound in Medicine & Biology 2004;30:229-37.

Browne JE, Watson AJ, Hoskins PR, Elliott AT. Investigation of the effect of subcutaneous fat on image quality performance of 2D conventional imaging and tissue harmonic imaging. Ultrasound in Medicine & Biology 2005;31:957-64.

Chen Q, Zagzebski JA. Simulation study of effects of speed of sound and attenuation on ultrasound lateral resolution. Ultrasound Med Biol 2004;30:1297-306.

D'Astous FT, Foster FS. Frequency-dependence of ultrasound attenuation and backscatter in breast-tissue. Ultrasound Med Biol 1986;12:795-808.

Del Grosso VA, Mader CW. Speed of sound in pure water. J Acoust Soc Am 1972;52:1442-6.

Dymling SO, Persson HW, Hertz CH. Measurement of blood perfusion in tissue using doppler ultrasound. Ultrasound Med Biol 1991;17:433-44.

Goldstein L. The effect of acoustic velocity on phantom measurements. Ultrasound Med Biol 2000;26:1133-43.

Goss SA, Johnston RL, Dunn F. Comprehensive compilation of empirical ultrasonic properties of mammalian-tissues. J Acoust Soc Am 1978;64:423-57.

Goss SA, Johnston RL, Dunn F. Compilation of empirical ultrasonic properties of mammalian-tissues .2. J Acoust Soc Am 1980;68:93-108.

IEC. Ultrasonics-Real-time pulse-echo systems-Guide for test procedures to determine performance specifications, IEC Publication 1390, Geneva: International Electrotechnical Commission. 1996;

Inglis S, Ramnarine KV, Plevris JN, McDicken WN. An anthropomorphic tissue-mimicking phantom of the oesophagus for endoscopic ultrasound. Ultrasound Med Biol 2006;32:249-59.

Pye SD, Ellis W, MacGillivray T. Medical ultrasound: a new metric of performance for grey-scale imaging. J Phys Conf Ser 2004;1:187-92.

Rosin M, Urban AD, GΣrtner C, Bernhardt O, Splieth C, Meyer G. Polymerization shrinkage-strain and microleakage in dentin-bordered cavities of chemically and light-cured restorative materials. Dental Materials 2002;18:521-8.

Scherzinger AL, Belgam RA, Carson PL, Meyer CR, Sutherland JV, Bookstein FL, Silver TM. Assessment of ultrasonic computed-tomography in symptomatic breast patients by discriminant-analysis. Ultrasound Med Biol 1988;15:21-8.

Shaw A, Hekkenberg R. Standards to support performance evaluation for diagnostic ultrasound imaging equipment, NPL Report AC 2, Teddington, UK: National. Physical Laboratory 2007;

Teirlinck CJPM, Bezemer RA, Kollmann C, Lubbers J, Hoskins PR, Ramnarine KV, Fish P, Fredfeldt KE, Schaarschmidt UG. Development of an example flow test object and comparison of five of these test objects, constructed in various laboratories. Ultrasonics 1998;36:653-60.

Wear KA, Stiles TA, Frank GR, Madsen EL, Cheng F, Feleppa EJ, Hall CS, Kim BS, Lee P, O'Brien WD, Oelze ML, Raju BI, Shung KK, Wilson TA, Yuan JR. Interlaboratory comparison of ultrasonic backscatter coefficient measurements from 2 to 9 MHz. J Ultras Med 2005;24:1235-50.

Welch PD. Use of fast Fourier transform for estimation of power spectra - A method based on time averaging over short modified periodograms. IEEE Trans Audio Electroacoust 1967;AU15:70-3.

Wells PNT. Ultrasound imaging. Phys Med Biol 2006;51:R83-R98.

Wells PNT. Absorption and dispersion of ultrasound in biological tissue. Ultrasound Med Biol 1975;1:369-76.

Zell K, Sperl JI, Vogel MW, Niessner R, Haisch C. Acoustical properties of selected tissue phantom materials for ultrasound imaging. Phys Med Biol 2007;52:N475-N484.

Figure Legends

Fig. 1. Cylindrical mould for TMMs

Fig. 2. Scanning acoustic macroscope configuration

Fig. 3. Attenuation coefficient of the NPL reference cell as a function of frequency

Fig. 4. Effect of glycerol concentration on the speed of sound (± 10 m. s^{-1}) of the TMMs

Fig. 5. Effect of glycerol concentration on the density and impedance of the TMMs

Fig. 6. Effect of SiC, Al_2O_3 (0.3 µm) and Al_2O_3 (3 µm) concentration on the attenuation coefficient (± 0.03 dB. cm^{-1}. MHz^{-1}) of the TMMs at 20 ºC

Fig. 7. Effect of SiC, Al_2O_3 (0.3 µm) and Al_2O_3 (3 µm) concentrations on relative backscatter (± 3 dB) of the TMMs at 20 ºC

Fig. 8. Effect of Al_2O_3 (0.3 µm and 3.0 µm) concentration on the attenuation coefficient (± 0.03 dB. cm^{-1}. MHz^{-1}) of the TMMs at 20 ºC

Fig. 9. Effect of SiC concentration on the attenuation coefficient

(± 0.03 dB. cm^{-1}. MHz^{-1}) of the TMMs at 20 ºC

Fig. 10. Effect of oil surfactant concentration on speed of sound (± 10 m. s^{-1}) of the TMMs at 20 ºC

Fig. 11. Effect of oil surfactant concentration on attenuation coefficient

(± 0.03 dB. cm^{-1}. MHz^{-1}) of the TMMs at 20 ºC

Fig. 12. Effect of oil surfactant concentration on the density and impedance of the TMMs

Appendix A

The attenuation measured for various tissues in the breast by D'Astous and Foster 1986 were fitted to curves of the form $\alpha(f) = \alpha_1 f^{\gamma}$, where α_1 represents the corresponding coefficients at 1MHz and γ represents the frequency dependence. Their data was presented in

dB. mm^{-1}. MHz^{-1} @ 1MHz. For this study the data was rescaled to dB. cm^{-1}. MHz^{-1} @ 7MHz. Rescaling was carried out as follows:

Fat

$0.0158 \pm 0.003\ dB.\ mm^{-1}.\ MHz^{-1}$ @ $1\ MHz$ with $\gamma = 1.7$
$Therefore\ \alpha = 0.0158 \times 7^{1.7}$
$\alpha = 0.4318\ dB.\ mm^{-1}$ @ $7MHz$
$\alpha = 4.3184\ dB.\ cm^{-1}$ @ $7MHz$
$\alpha = 0.6169\ dB.\ cm^{-1}.\ MHz^{-1}$ @ $7MHz$

IDC

$0.0570 \pm 0.014\ dB.\ mm^{-1}.\ MHz^{-1}$ @ $1\ MHz$ with $\gamma = 1.3$
$Therefore\ \alpha = 0.0570 \times 7^{1.3}$
$\alpha = 0.7153\ dB.\ mm^{-1}$ @ $7MHz$
$\alpha = 7.1532\ dB.\ cm^{-1}$ @ $7MHz$
$\alpha = 1.0219\ dB.\ cm^{-1}.\ MHz^{-1}$ @ $7MHz$

Glandular

$0.0870 \pm 0.029\ dB.\ mm^{-1}.\ MHz^{-1}$ @ $1\ MHz$ with $\gamma = 1.5$
$Therefore\ \alpha = 0.0870 \times 7^{1.5}$
$\alpha = 1.61126\ dB.\ mm^{-1}$ @ $7MHz$
$\alpha = 16.1126\ dB.\ cm^{-1}$ @ $7MHz$
$\alpha = 2.3018\ dB.\ cm^{-1}.\ MHz^{-1}$ @ $7MHz$